Geomechanics and Engineering, *Vol. 6, No. 3 (2014) 263-275*
DOI: http://dx.doi.org/10.12989/gae.2014.6.3.263

2D numerical investigations of twin tunnel interaction

Ngoc Anh Do [*1,4], Daniel Dias [2], Pierpaolo Oreste [3] and Irini Djeran-Maigre [1]

[1] *Laboratory LGCIE, University of Lyon, INSA of Lyon, Villeurbanne, France*
[2] *Laboratory LTHE, Grenoble Alpes University, Grenoble, France*
[3] *Department of Environmental, Land and Infrastructural Engineering, Politecnico of Torino, Torino, Italy*
[4] *Department of Underground and Mining Construction, Faculty of Civil Engineering, Hanoi University of Mining and Geology, Vietnam*

(*Received February 10, 2013, Revised October 20, 2013, Accepted October 26, 2013*)

Abstract. The development of transportation in large cities requires the construction of twin tunnels located at shallow depth. As far as twin tunnels excavated in parallel are concerned, most of the cases reported in literature focused on considering the effect of the ground condition, tunnel size, depth, surface loads, the relative position between two tunnels, and construction process on the structural lining forces. However, the effect of the segment joints was not taken into account. Numerical investigation performed in this study using the FLAC^{3D} finite difference element program made it possible to include considerable influences of the segment joints and tunnel distance on the structural lining forces induced in twin tunnels. The structural lining forces induced in the first tunnel through various phases are considerably affected by the second tunnel construction process. Their values induced in a segmental lining are always lower than those obtained in a continuous lining. However, the influence of joint distribution in the second tunnel on the structural forces induced in the first tunnel is insignificant. The critical influence distance between two tunnels is about two tunnel diameters.

Keywords: tunnel; twin tunnels; segmental lining; structural forces; segmental joint; tunnel distance; numerical model

1. Introduction

Many tunnelling projects have recently been constructed that involve the excavation of twin tunnels in close proximity to each other. Even if in many cases, the new tunnel was excavated at close distance to an existing tunnel. Therefore, it is very important to understand in detail the interaction mechanism between two tunnels during their construction processes. Obviously, the interaction between two adjacent tunnels is complex, which depends on many factors such as geometry of tunnels, lining properties, ground characteristics, and construction methods.

For the construction of urban underground tunnels in soft ground, shield-driven tunnelling method is widely adopted due to its flexibility, cost effectiveness and its small impact on the ground surface. Segmental concrete lining is commonly used in most shield-driven tunnels which generally comprises a sequence of rings placed side-by-side (Gruebl 2006).

∗Corresponding author, Ph.D. Student, E-mail: ngoc-anh.do@insa-lyon.fr

http://www.techno-press.org/?journal=gae&subpage=7 ISSN: 2005-307X (Print), 2092-6219 (Online)

The main difference between a segmental lining and a continuous lining is the existence of the joints in the segmental lining. Under the influence of the joints, the behaviour of the segmental lining will be different from the one induced in a continuous lining.

In the literature, some numerical models that introduced the effect of the segment joints on the tunnel lining behaviour (Hefny *et al*. 2006, Teachvorasinskun and Chub-Uppakarn 2010, Do *et al*. 2013a, b, c and d) were developed. However, these models focused only on a single tunnel. As far as the twin tunnels excavated in parallel are concerned, most of the reported cases considered the effect of the ground condition, tunnel size, depth, surface loads, relative position between two tunnels, and construction process on the structural forces (Hefny *et al*. 2004, Ng *et al*. 2004, Hage Chehade and Shahrour 2008, Afifipour *et al*. 2011, etc.). Nevertheless, the effect of the segment joints was not taken into considered.

Two-dimensional (2D) numerical investigation performed in this study made it possible to include considerable influences of segment joint and distance between two tunnels on the structural forces induced in both tunnels. The results showed that the critical influence distance between two tunnels is about two tunnel diameters. The structural lining forces induced in the first tunnel through various phases are considerably affected by the second tunnel construction process. Their values induced in a segmental lining are always lower than the ones developed in a continuous lining. However, the influence of the joint distribution in the second tunnel on the structural lining forces induced in the first tunnel is insignificant.

2. Numerical modelling

When tunnelling process is performed in 2D plane strain model, an assumption that takes into account the pre-displacement of the ground surrounding the tunnel boundary prior to the installation of structural elements must be adopted. This pre-displacement process of the tunnel wall is called hereafter the deconfinement process. The available equivalent approaches, that allow the deconfinement process to be controlled, include the convergence confinement method (CCM) (Panet and Guenot 1982, Oreste 2003), gap method (Rowe *et al*. 1983), progressive softening method (Swoboda 1979), volume loss method (VLM) (Bernat 1996, Hejazi *et al*. 2008), and grout pressure method (Möller and Vermeer 2008). Apart from the VLM, gap method, and grouting pressure method, Karakus (2007) used various ways of tunnel excavation modelling, that take into account three-dimensional (3D) effects in a 2D model, to determine the shape of the settlement trough on the ground surface. This work shows that the CCM allows the best agreement with experimental results. Do *et al*. (2013b) performed numerical investigations that compare 2D numerical analyses using both the VLM and the CCM with 3D numerical analyses. Their results indicated that the structural lining forces determined with the CCM are in better agreement with the 3D numerical results than those obtained with the VLM. For the above reasons, the CCM has been adopted in this study.

The determination of the ground convergence, when the support system becomes active, is an essential element of the CCM. This method is also known as the "λ_d method". Choosing a value of the stress release ratio λ_d before the lining being installed is one of the difficulties when applying this method. In this study, for the purpose of the numerical investigation, a λ_d value of 0.3 has been adopted (Möller and Vermeer 2008).

In order to avoid a possible soil decompression that relates to the annular void appearing between the excavated soil surface and the concrete lining, the tail void grouting is performed. In general, after being injected into the void behind the shield tail, the grouting action are modelled through two phases: (1) the liquid state (state 1) represented by a certain pressure simultaneously acting on both the soil surface and the tunnel lining; (2) the solid state (state 2) (Melis *et al*. 2002, Kasper and Meschke 2004, Mollon *et al*. 2013).

As far as the grouting pressure distribution over the tunnel height is concerned, there is no a unique rule that is accepted by all researchers (Rijke 2006). However, the distribution of the grouting pressure can be generally assumed to be linearly increased with depth under the grout unit weight effect (Bezuijen and Talmon 2004). In this study, the vertical grouting pressure gradient behind the TBM is assumed to be of 15 kPa/m, which corresponds to the density of the fresh grout. The grout pressure applied to the tail void is generally set to (Mollon *et al*. 2013)

$$\sigma_{inj} = 1.2 \cdot \sigma_v \tag{1}$$

where σ_v is the soil overburden pressure at the tunnel crown.

Fig. 1 shows a 2D numerical model which utilizes the plane-strain conditions. Parameters from the Bologna-Florence high-speed railway line tunnel project have been adopted in this numerical modelling as the reference case (Croce 2011) (see Table 1).

The tunnel structure behaviour is assumed to be elastic linear. The soil behaviour is assumed to be governed through a linear elastic perfectly-plastic constitutive relation based on the Mohr-Coulomb failure criterion.

In this study, numerical simulations have been performed by means of the FLAC^{3D} finite difference element program (Itasca 2009), which provides flexible features for the analyses of joint parameters. The volume under study has been discretized into hexahedral zones. The tunnel segments have been modelled using the embedded liner elements (e.g., Do *et al*. 2012, Do *et al*. 2013a, b, c and d). These elements are used to model thin liners (based on the classical Kirchhoff plate theory) for which both normal-directed compressive/tensile interaction and shear-directed frictional interaction with the host medium occurs (Itasca 2009). Some typical tunnel lining parameters are summarized in Table 1.

As described by Do *et al*. (2013a), the segment joints have been simulated using double node connections (Fig. 2). These include six degrees of freedom, which are represented by six springs: three translational components in the *x*, *y* and *z* directions , and three rotational components around

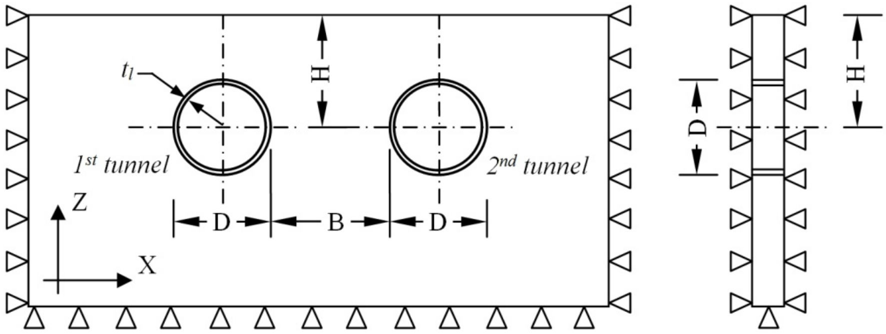

Fig. 1 Plane strain model under consideration (not scaled)

Table 1 Details of the reference case

Parameter	Symbol	Value	Unit
Properties of clayey sand			
Unit weight	γ_S	17	kN/m^3
Young's modulus	E_S	150	MPa
Poisson's ratio	ν_S	0.3	-
Internal friction angle	φ_S	37	degrees
Cohesion	c	0	kPa
Lateral earth pressure coefficient at rest	K_0	0.5	-
Overburden	H	20	m
Properties of tunnel lining			
Young's modulus	E_l	35	GPa
Poisson's ratio	ν_l	0.15	-
Lining thickness	t_l	0.4	m
External diameter	D	9.4	m
Tunnel distance	B	varied	-
Properties of grouting layer			
Young's modulus	E_g	10	MPa
Poisson's ratio	ν_g	0.22	-
Grouting layer thickness	t_g	0.15	m
Grout density	γ_g	15	kN/m^3

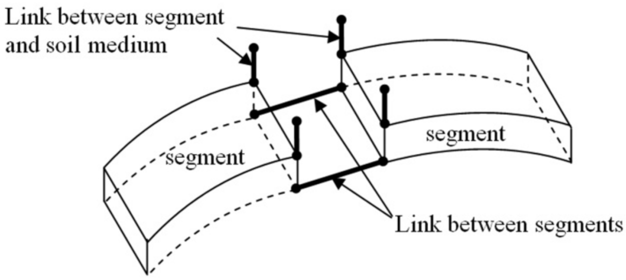

Fig. 2 Joint connection scheme (Do *et al*. 2013a)

the x, y and z directions. In this study, the stiffness characteristics of the joint connection are represented by a set composed of a rotational spring (K_θ), an axial spring (K_A) and a radial spring (K_R), as depicted in Fig. 3. As described by Do *et al*. (2013a), on the basis the basic of empirical data (Cavalaro and Aguado 2011), the behaviour of axial springs has been represented by a linear relation using a constant coefficient spring. The radial stiffness and rotational stiffness of a segment joint have instead been modelled by means of a bi-linear relation that is characterized by a stiffness factor and maximum bearing capacity. The attachment conditions of the translational

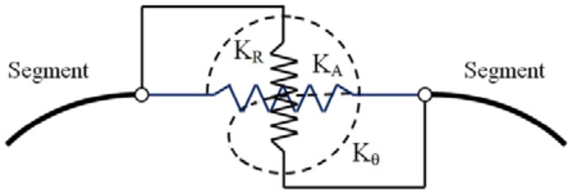

Fig. 3 K_A, K_R, K_θ stiffnesses in the axial, radial and rotational directions of a segment joint (Do *et al*. 2013a)

component in the *y* direction, which is parallel to the longitudinal axis of the tunnel, and two rotational components around the *x* and *z* directions are assumed to be rigid for all the investigated cases (Do *et al*. 2013a, b and c).

The values of the spring constants used to simulate the segment joints have been determined on the basis of the simplified procedures presented by Thienert and Pulsfort (2011) and Do *et al*. (2013a). The numerical study performed by Do *et al*. (2013a) showed an insignificant influence of the axial and radial stiffness of the joints on segmental tunnel lining behaviour. On the other hand, the effect of rotational stiffness was considerable. The segment joint parameters are presented in Table 2.

As described by Do *et al*. (2013a), embedded liner elements are attached to the zone faces along the tunnel boundary. The liner-zone interface stiffness (normal stiffness k_n and tangential stiffness k_s) is chosen using a rule-of-thumb in which k_n and k_s are set to one hundred times the equivalent stiffness of the stiffest neighboring zone (Itasca 2009). The apparent stiffness (expressed in stress-per-distance units) of a zone in the direction normal to the surface is

$$\max\left[\frac{\left(K+\frac{4}{3}G\right)}{\Delta z_{\min}}\right] \tag{2}$$

where: K and G are the bulk and shear modulus, respectively;

$z_{\min}$ is the smallest dimension of an adjoining zone in the normal direction.

The FLAC^{3D} model grid contains a single layer of zones in the y-direction, and the dimension of elements increases as one moves away from the tunnel (see Fig. 4). The numerical model is 60 m high in the *z*-direction. The width in the x-direction is varied depending on the distance between two tunnels.

Table 2 Parameters of the segment joints

Rotational stiffness K_θ (MN.m/rad/m)	100
Maximum bending moment at segment joint M_{yield} (kN.m/m)	150
Axial stiffness K_A (MN/m)	500
Radial stiffness K_R (MN/m)	1050
Maximum shear forces at segment joint S_{yield} (MN/m)	0.55

Modelling of the construction process of the two tunnels has been carried out in the following steps:

- Setting up the model of two tunnels, assigning the plane strain boundary conditions and the initial gravity stress state;
- Constructing the first tunnel that includes three phases as follows:
  + 1st phase: Deactivating the excavated ground, simultaneously applying a stress relaxation ratio λ_d of 0.3 to the tunnel boundary (Fig. 5);
  + 2nd phase: Activating the segments in a ring, assigning joint stiffnesses; simultaneously applying the total relaxation, and setting up the grouting pressure, which acts over the whole tunnel periphery, on both tunnel structure and ground surface.
  + 3rd phase: Consolidation of the grout: the hardened grout in the present model has been simulated by means of volume elements with perfect elastic behaviour, and with the elastic characteristics E_{grout} = 10 MPa and ν_{grout} = 0.22 (Mollon *et al*. 2013, Do *et al*. 2013c and d).
- Starting the construction of the second tunnel using the same procedure as performed for the first tunnel, which includes three phases ordered as the 4th phase, 5th phase, and 6th phase, respectively, in this study.

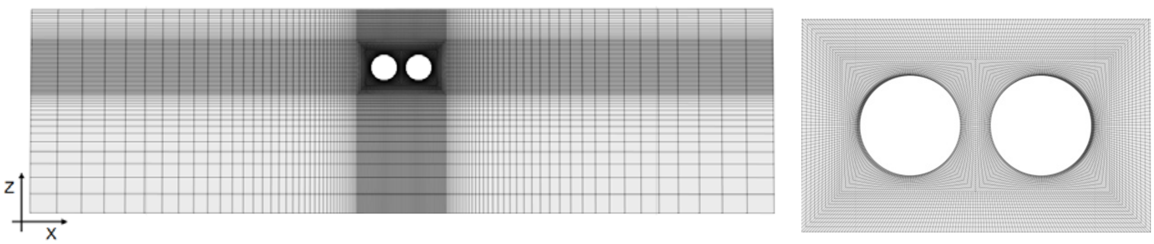

(a) (b)

Fig. 4 (a) 2D numerical model; (b) zoom of twin tunnels in case of tunnel distance B = 0.25 D

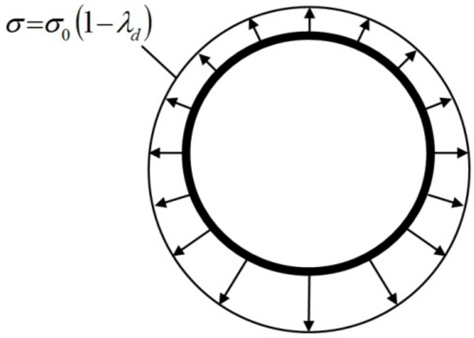

Fig. 5 Tunnelling simulation by the λ_d method (Hejazi *et al*. 2008)

3. Parametric investigation

3.1 Impact of the second tunnel construction process on the first tunnel structure behaviour

The reference case (Table 1) with a joint number of 6 has been adopted in this study. Segment joints in the first tunnel are fixed at angles of 0°, 60°, 120°, 180°, 240°, and 300° measured counter-clockwise spring line on the right. On the other hand, segment joint locations in the second tunnel have been changed in order to determine the effect of the joint distribution on the first tunnel behaviour.

For each tunnel distance value (B) which changes over a range from 0.25 D to 3 D, the numerical results, which are not presented in figures in this paper, show that the joint distribution in the second tunnel has a negligible influence on both normal force and bending moment induced in the first tunnel. For this reason, all the other calculations performed in this study have conducted using a set of the segment joints in the second tunnel that are fixed at the same angle as those in the first tunnel mentioned above.

In this section, the bending moment ratio, R_M, and the normal force ratio, R_N, which are not graphed in the figures, are defined as the ratio of the maximum absolute value of the bending moment and normal force, respectively, induced in the lining of the first tunnel, that are determined at the 6th phase, to the corresponding ones developed in the first tunnel lining at the 3rd phase. It should be noted that the behaviour of the first tunnel determined at the 3rd phase can be considered as that of a single tunnel. The maximum values of the normal force and maximum/minimum values of the bending moment are presented in Figs. 6, 7 and 8, respectively.

Fig. 6 shows that the normal forces induced in both the jointed and continuous linings of the first tunnel, determined at the 6th phase, are considerably affected by the tunnel distance. As expected, the greater the tunnel distance, the lower the impact of the second tunnel on the normal force induced in the first tunnel. It should be noted that the normal force ratio R_N in a jointed lining is greater than that of a continuous lining when the tunnel distance is less than 1 D. This means that the jointed lining in the first tunnel is more sensitive to the impact of the second tunnel construction than a continuous lining.

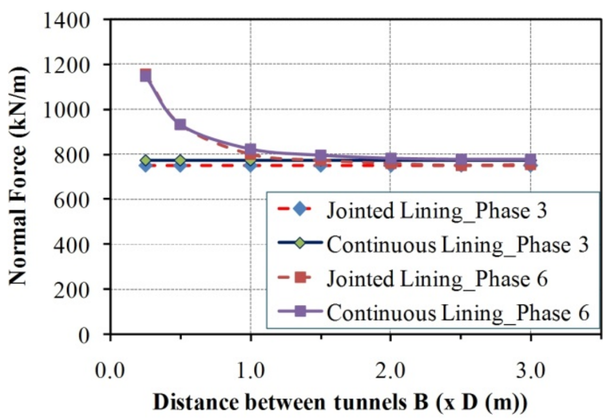

Fig. 6 Maximum normal force induced in the first tunnel

Also at a tunnel distance that is less than 1 D, Fig. 6 presents a great impact of the second tunnel construction on the first tunnel, represented by high values of the R_N ratio. Generally, the magnitude of the normal forces induced in the first tunnel, after being interacted with the second tunnel, is greater than the one developed in a single tunnel. This suggests that an increase in the external load acting on the first tunnel was expected due to the excavation of the second tunnel. At a tunnel distance of about 2 D, the R_N ratios, determined in both cases in which the jointed lining and continuous lining are used, are approximately unity (Fig. 6). This means that, beyond this distance, the influence of the second tunnel construction process on the first tunnel behaviour, in terms of the normal forces, can be neglected.

Figs. 7 and 8 presents a considerable influence of the tunnel distance on the bending moment induced in both jointed and continuous linings of the first tunnel. When the tunnel distance is less than 1 D, an increase in the tunnel distance would result in a reduction in the absolute bending moment, determined at the 6th phase, in the first tunnel. This is consistent with the numerical results performed by Hossani *et al*. (2012). Beyond this distance, the results show a negligible

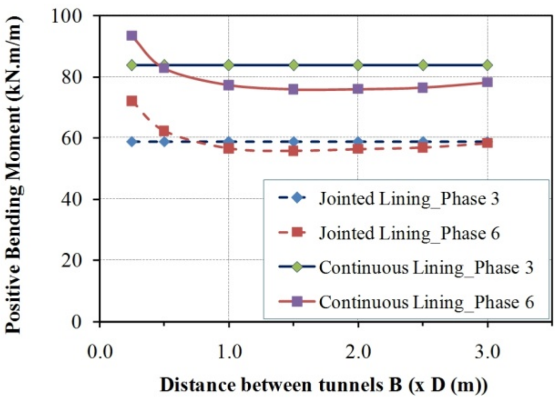

Fig. 7 Maximum positive bending moment induced in the first tunnel

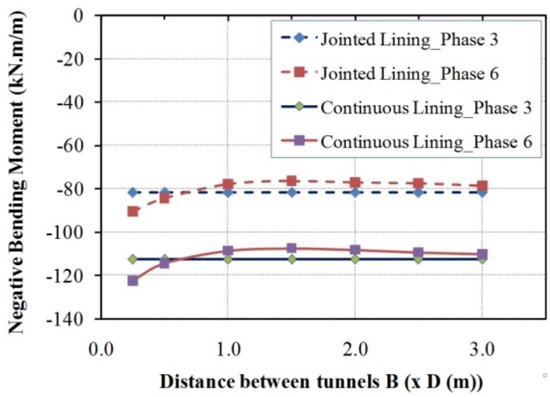

Fig. 8 Minimum negative bending moment induced in the first tunnel

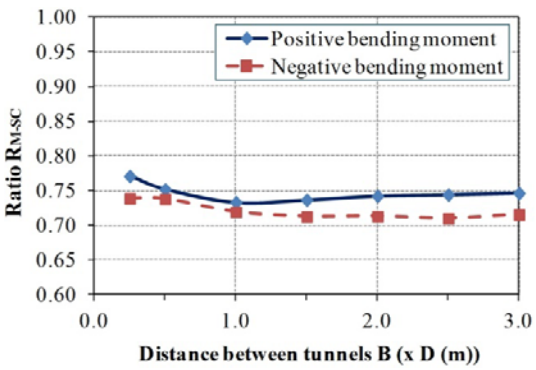

Fig. 9 Influence of the tunnel distance on the ratio $R_{M\text{-}SC}$

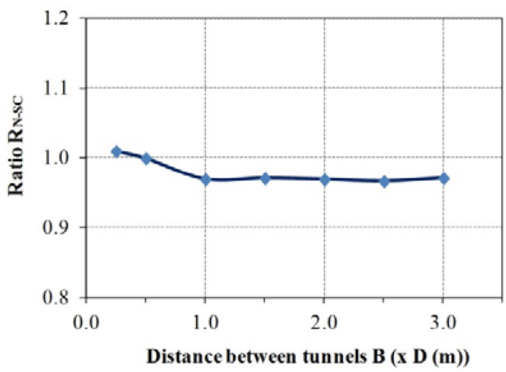

Fig. 10 Influence of the tunnel distance on the ratio $R_{N\text{-}SC}$

variation in the bending moment induced in the first tunnel. It should be noted that, at a tunnel distance that is less than about 0.5 D, the bending moment ratio R_M is generally higher than unity. However, beyond this distance, the R_M value is always smaller than unity.

Figs. 9 and 10 show the effect of the tunnel distance on the $R_{M\text{-}SC}$ and $R_{N\text{-}SC}$ ratios, which are defined as the ratio of the bending moment and normal force, respectively, induced in a jointed lining in the first tunnel, to the corresponding ones induced in a continuous lining. All of these structural lining forces were determined at the 6th phase. It should be noted that the bending moment induced in a jointed lining is always smaller than the one developed in a continuous lining due to the influence of the segment joints. The ratio $R_{M\text{-}SC}$ changes over a range from 0.715 to 0.742 and from 0.735 to 0.77, corresponding to the negative bending moment and positive bending moment. However, the normal forces seem to be not significantly affected by the segment joints. Indeed, the $R_{N\text{-}SC}$ ratio changes over a range from 0.969 to 1.001.

3.2 Impact of the first tunnel construction process on the second tunnel structure behaviour

Figs. 11 to 15 present the dependence of the structural lining forces induced in the two tunnels on the tunnel distance. The R_{M21} and R_{N21} ratios are defined as the ratio of the bending moment and normal force, respectively, induced in the second tunnel to the corresponding ones developed in the first tunnel. All of them were determined at the 6th phase.

As can be seen in Fig. 11, due to the impact of the first tunnel excavation, the normal force developed in the second tunnel is generally higher than that induced in the first tunnel measured at the 3rd phase, which corresponds to the behaviour of a single tunnel, especially at a tunnel distance (B) which is less than 1 D. The maximum differences of about 22.3 % and 21.6 % corresponding to the cases of a jointed lining and a continuous lining were obtained at a tunnel distance of 0.25 D (Fig. 11).

Fig. 12 shows that the normal force in the second tunnel lining is generally smaller than that in the first tunnel lining determined at the 6th phase. The R_{N21} ratio is usually less than unity. This suggests that more loads are taken by the first tunnel than by the second tunnel. Similar observations were also obtained through 3D numerical analyses of twin new Austrian tunnelling

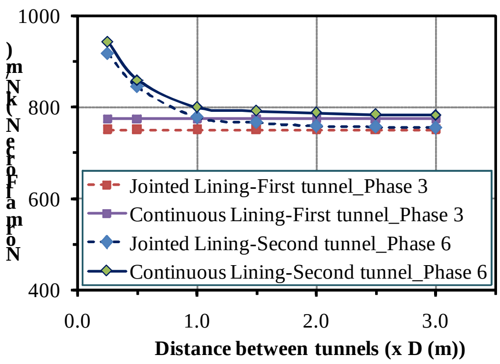

Fig. 11 Maximum normal force induced in the second tunnel

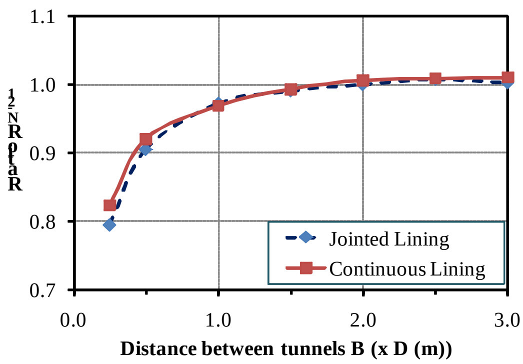

Fig. 12 Influence of the tunnel distance on the ratio R_{N21}

method tunnels performed by Ng *et al*. (2004). For a jointed lining, the R_{N21} ratio is generally smaller than that of a continuous lining. In other words, compared to the case of continuous lining, greater difference between the normal forces induced in two parallel tunnels supported by jointed linings is expected.

Figs. 11 and 12 also show that the impact between two tunnels is more considerable when the tunnel distance (B) is less than 1 D. At a tunnel distance of about 2 D, the R_{N21} ratios determined in both cases in which jointed and continuous linings are used are approximately unity. One again, it is possible to conclude that, beyond this distance, the impact between two tunnels excavated in parallel, in terms of the normal force, can be ignored. This conclusion is in good agreement with the results obtained in the Hage Chehade and Shahrour (2008) study, which was also performed using a 2D model. In their study, the critical distance of the influence between two tunnels was determined on the basis of the settlement trough that developed on the ground surface. However, different from the results in Hage Chehade and Shahrour (2008) study, in which the bending moment and normal forces induced in the second tunnel were negligibly affected by the tunnel distance, a strong dependence of the normal forces induced in the second tunnel on the distance between two tunnels that obtained in this study has been shown. The above difference could be attributed to the fact that, unlike the numerical model in this paper, the effect of the grouting pressure and segment joints was not taken into consideration in the study of Hage Chehade and Shahrour (2008).

Figs. 13 and 14 present the bending moment in both tunnels determined at the 3rd and 6th phases, respectively. The behaviour of the first tunnel determined at the 3rd phase can be considered as that of a single tunnel. Fig. 13 shows that the positive bending moment in the second tunnel is generally smaller than that developed in a single tunnel. Whereas, apart from the tunnel distance which is greater than 0.5 D, the absolute negative bending moment in the second tunnel is greater than the one induced in a single tunnel (Fig. 14). The maximum difference of the bending moment determined in the two tunnels is about 7%.

As the tunnel distance is lower than 0.75 D, the R_{M21} ratio is generally lower than unity. This means that for this range of the tunnel distance, the bending moments in the first tunnel are greater than that of the second tunnel (Fig. 15). In contrary, beyond the tunnels distance of 0.75 D, the R_{M21} ratio is generally higher than unity.

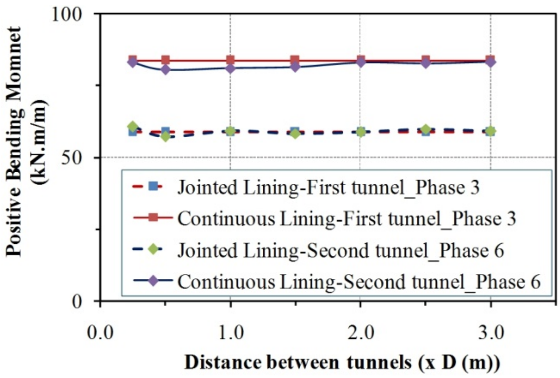

Fig. 13 Maximum positive bending moment induced in the second tunnel

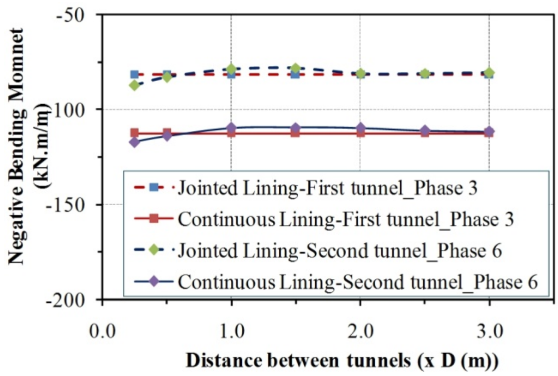

Fig. 14 Minimum negative bending moment induced in the second tunnel

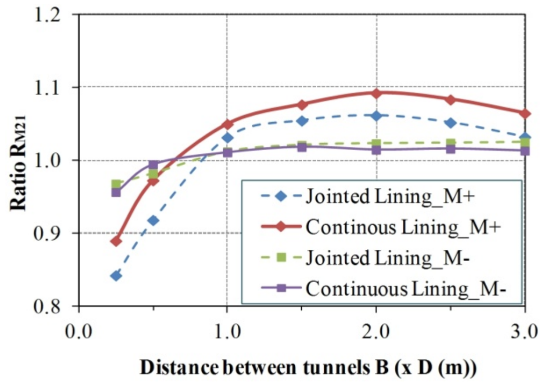

Fig. 15 Influence of the tunnel distance on the ratio R_{M21}

When the tunnel distance is less than 1 D, an increase in the tunnel distance will result in a significant increase in the R_{M21} ratio determined in both cases of jointed and continuous linings. Apart from the tunnel distance which is less than 1 D, the negative bending moment ratio determined at the tunnel side wall (due to the K_0 value of 0.5 in this reference case) is not sensitive to the change in the tunnel distance.

4. Conclusions

This paper presented 2D numerical analyses of twin tunnels excavated in close proximity in order to investigate the influence of both the segment joints and tunnel distance on the structural forces induced in the tunnel lining. The impact of the second tunnel construction process on the first tunnel, and vice versa, in terms of the bending moment and normal force, has been discussed. The numerical investigation has shown a considerable effect of the segment joints and tunnel distance on the behaviour of both tunnels.

Owing to the excavation of the second tunnel, an increase in the external load acting on the first tunnel was expected. The greater the tunnel distance, the lower the impact of the second tunnel on the normal force in the first tunnel. A jointed lining in the first tunnel is more sensitive to the impact of the second tunnel construction than a continuous lining. At a tunnel distance of about 2 D, the variation in the normal forces induced in the first tunnel due to the impact of the second tunnel, for both cases in which the tunnel is supported by jointed lining and continuous lining, can be ignored.

When the tunnel distance is less than 1 D, an increase in the tunnel distance would result in a reduction in the absolute bending moment determined at the 6^{th} phase in the first tunnel. Beyond this distance, the results show a negligible variation in the bending moment induced in the first tunnel.

The variation in the joint distribution in the second tunnel has a negligible influence on both normal force and bending moment induced in the first tunnel.

Due to the impact of the first tunnel excavation, the normal force in the second tunnel is generally higher than that induced in a single tunnel, especially at tunnel distance which is less than 1 D. However, the normal force determined at the 6th phase in the second tunnel is generally smaller than that induced in the first tunnel. The R_{N21} ratio is usually less than unity. For a jointed lining, the R_{N21} ratio is always smaller than that of a continuous lining.

Generally, the results show that the impact between two tunnels is more considerable when the tunnel distance is less than 1 D. At a tunnel distance of about 2 D, the impact of the first tunnel construction process on the second tunnel behaviour can be negligible.

Above results made it possible to conclude that beyond a tunnel distance of 2 D, the impact between two tunnels excavated in close proximity, in terms of the normal force, can be ignored.

The results obtained from this study are believed to be useful for design considerations of closely spaced bored tunnels. Further comparisons with experimental data, obtained from a real tunnel excavation, should be made in order to improve the quality of the numerical simulation.

References

Afifipour, M., Sharifzadeh, M., Shahriar, K. and Jamshidi, H. (2011), "Interaction of twin tunnels and shallow foundation at Zand underpass, Shiraz metro, Iran", *Tunn. Undergr. Sp. Tech.*, **26**(2), 356-363.

Bernat, S. (1996), "Modélisation des déformations induites par le creusement d'un tunnel - Application au métro de Lyon-Vaise", Ph.D. Dissertation, Ecole Centrale de Lyon. [In French]

Bezuijen, A. and Talmon, A.M. (2004), "Grout pressures around a tunnel lining, influence of grout consolidation and loading on lining", *Proceedings of World Tunnel Congress and 13th ITA Assembly*, Singapore, May; *Tunnel. Undergr. Space Tech.*, **19**, 443-444.

Cavalaro, S.H.P. and Aguado, A. (2011), "Packer behaviour under simple and coupled stresses", *Tunn. Undergr. Sp. Tech.*, **28**, 159-173.

Croce, A. (2011), "Analisi dati di monitoraggio del rivestimento della galleria del passante ferroviario di Bologna", Degree Dissertation, Polytechnics of Torino, Italy. [In Italian]

Do, N.A., Dias, D., Oreste, P.P. and Djeran-Maigre, I. (2012), "Numerical investigation of surface settlement above a tunnel: Influence of segmental joints and deformability of ground", *Proceeding of 2nd International Conference on Advances in Mining and Tunnelling*, Vietnam, ISBN: 978-604-913-081-6, pp. 251-258.

Do, N.A., Dias, D., Oreste, P.P. and Djeran-Maigre, I. (2013a), "2D numerical investigation of segmental tunnel lining behavior", *Tunn. Undergr. Sp. Tech.*, **37**, 115-127.

Do, N.A., Dias, D., Oreste, P.P. and Djeran-Maigre, I. (2013b), "2D tunnel numerical investigation - The influence of the simplified excavation method on tunnel behaviour", *Geotech. Geol. Eng.*, **32**(1), 43-58. DOI: http://dx.doi.org/10.1007/s10706-013-9690-y

Do, N.A., Dias, D., Oreste, P.P. and Djeran-Maigre, I. (2013c), "3D modelling for mechanized tunnelling in soft ground - Influence of the constitutive model", *Am. J. Appl. Sci.*, **10**(8), 863-875, DOI: http://dx.doi.org/10.3844/ajassp.2013.863.875

Do, N.A., Dias, D., Oreste, P.P. and Djeran-Maigre, I. (2013d), "Three-dimensional numerical simulation for mechanized tunnelling in soft ground – The influence of the joints", *Acta Geotech.*, p. 1. DOI: http://dx.doi.org/10.1007/s11440-013-0279-7

Gruebl, F. (2006), "Modern design aspects of segmental lining", *CPT-ITA Congress*.

Hage Chehade, F. and Shahrour, I. (2008), "Numerical analysis of the interaction between twin-tunnels: Influence of the relative position and construction procedure", *Tunn. Undergr. Sp. Tech.*, **23**(2), 210-214.

Hefny, A.M., Chua, H.C. and Jhao, J. (2004), "Parametric studies on the interaction between Existing and new bored tunnels", *Tunn. Undergr. Sp. Tech.*, **19**(4-5), 471.

Hefny, A.M. and Chua, H.C. (2006), "An investigation into the behaviour of jointed tunnel lining", *Tunn. Undergr. Sp. Tech.*, **21**(3-4), 428.

Hejazi, Y., Dias, D. and Kastner, R. (2008), "Impact of constitutive models on the numerical analysis of

underground constructions", *Acta Geotech*., **3**(4), 251-258.
Hossaini, S.M.F., Shaban, M. and Talebinejad, A. (2012), "Relationship between twin tunnels distance and surface subsidence in soft ground of Tabriz metro – Iran", *The 12th Coal Operator's Conference*, University of Wollongong & The Australasian Institute of Mining and Metallurgy, pp. 163-168.
Itasca Consulting Group, Inc. (2009), *FLAC Fast Lagrangian Analysis of Continua*, Version 4.0, User's manual. http://itascacg.com
Karakus, M. (2007), "Appraising the methods accounting for 3D tunnelling effects in 2D plane strain FE analysis", *Tunn*. *Undergr*. *Sp*. *Tech*., **22**(1), 47-56.
Kasper, T. and Meschke, G. (2004), "A 3D finite element simulation model for TBM tunnelling in soft ground", *Int*. *J*. *Numer*. *Anal*. *Method*. *Geomech*., **28**(14), 1441-1460.
Melis, M., Medina, L. and Rodriguez, J.M. (2002), "Prediction and analysis of subsidence induced by shield tunnelling in the Madrid Metro extension", *Canadian Geotechnical Journal*, **39**, 1273-1287.
Möller, S.C. and Vermeer, P.A. (2008), "On numerical simulation of tunnel installation", *Tunn*. *Undergr*. *Sp*. *Tech*,**23**, 461-475.
Mollon, G., Dias, D. and Soubra, A.H . (2013), "Probabilistic analyses of tunnelling-induced ground movements", *Acta Geotechnica*, DOI 10.1007/s11440-012-0182-7.
Ng, C.W.W, Lee, K.M. and Tang, D.K.W. (2004), "Three-dimensional numerical investigations of new Austrian tunnelling method (NATM) twin tunnel interactions", *Can*. *Geotech*. *J*., **41**(3), 523-539.
Oreste, P.P. (2003), "Analysis of structural interaction in tunnels using the convergence – Confinement approach", *Tunn*. *Undergr*. *Sp*. *Tech*., **18**(4), 347-363
Panet, M. and Guenot, A. (1982), "Analysis of convergence behind the face of a tunnel", *Proceedings of the International Symposium*, *Tunnelling-82*, 187-204.
Rijke, Q.C. (2006), "Innovation of stress and damage reduction in bored tunnels during construction based on a shield equilibrium model", Ph.D. Dissertation, Utrecht, Delft University of Technology and Holland Railconsult, February.
Rowe, R.K., Lo, K.Y. and Kack, K.J. (1983), "A method of estimating surface settlement above shallow tunnels constructed in soft ground", *Can*. *Geotech*. *J*., **20**(1), 11-22.
Swoboda, G. (1979), "Finite element analysis of the New Austrian Tunnelling Method (NATM)", *Proceedings of the 3rd International Conference on Numerical Methods Geomechanics*, Aachen, April, Vol. **2**, p. 581.
Teachavorasinskun, S. and Chub-Uppakarn, T. (2010), "Influence of segmental joints on tunnel lining", *Tunn*. *Undergr*. *Sp*. *Tech*., **25**(4), 490-494.
Thienert, C. and Pulsfort, M. (2011), "Segment design under consideration of the material used to fill the annular gap", *Geomech*. *Tunn*., **4**, 665-680.

CC